

Tuning the Triplet Energy Levels of Pyrazolone Ligands to Match the 5D_0 Level of Europium(III)

Mei Shi,[†] Fuyou Li,^{*,†} Tao Yi,[†] Dengqing Zhang,[†] Huaiming Hu,[‡] and Chunhui Huang^{*,†}

Laboratory of Advanced Materials, Fudan University, Shanghai 200433, P. R. China, and
Department of Chemistry, Northwest University, Xi'an 710069, P. R. China

Received May 25, 2005

Three pyrazolone-based ligands, namely 1-phenyl-3-methyl-4-(1-naphthoyl)-5-pyrazolone (**HL1**), 1-phenyl-3-methyl-4-(4-dimethylaminobenzoyl)-5-pyrazolone (**HL2**), and 1-phenyl-3-methyl-4-(4-cyanobenzoyl)-5-pyrazolone (**HL3**), were synthesized by introducing electron-poor or electron-rich aryl substituents at the 4-position of the pyrazolone ring. Their corresponding europium complexes $\text{Eu}(\text{LX})_3(\text{H}_2\text{O})_2$ and $\text{Eu}(\text{LX})_3(\text{TPPO})(\text{H}_2\text{O})$ ($X = 1-3$) were characterized by photophysical studies. The characteristic Eu(III) emission of these complexes with at most 9.2×10^{-3} of fluorescent quantum yield was observed at room temperature. The results show that the modification of ligands tunes the triplet energy levels of three pyrazolone-based ligands to match the 5D_0 energy level of Eu^{3+} properly and improves the energy transfer efficiency from antenna to Eu^{3+} , therefore enhancing the Eu(III) emission intensity. The highest energy transfer efficiency and probability of lanthanide emission of $\text{Eu}(\text{L1})_3(\text{H}_2\text{O})_2$ are 35.1% and 2.6%, respectively, which opens up broad prospects for improving luminescent properties of Eu(III) complexes by the modification of ligands. Furthermore, the electroluminescent properties of $\text{Eu}(\text{L1})_3(\text{TPPO})(\text{H}_2\text{O})$ were also investigated.

Introduction

On the basis of the unique photophysical properties of lanthanide cations (long luminescence lifetime and very sharp emission band),¹ rare earth metal complexes, especially europium(III) complexes, as luminescent materials have received increasing attention for application in bioassays² and sensor systems.³ It is well-known that the application of the strong absorbing “antennae” for light harvesting is required for the low extinction coefficients of the lanthanide ions. The β -diketone ligand is one kind of important

“antenna”, from which the energy can be effectively transferred to Eu(III) and Tb(III) ions for high harvest emissions.^{4–6} For example, the terbium complexes based on the pyrazolone-based ligands 1-phenyl-3-methyl-4-isobutyryl-5-pyrazolone (**HL4**)⁷ and 1-phenyl-3-methyl-4-(2-ethylbutyryl)-5-pyrazolone (**HL5**)⁸ (see Chart 1) can emit characteristic Tb(III) photoluminescence with high quantum yield.

Recently, europium complexes have attracted more interest in organic light-emitting diodes (OLED) for their saturated red-emission.^{5,9–17} Although several europium complexes have been applied as red emitters in electroluminescent (EL) devices, their ligands are mainly limited to 1,3-diphenyl-

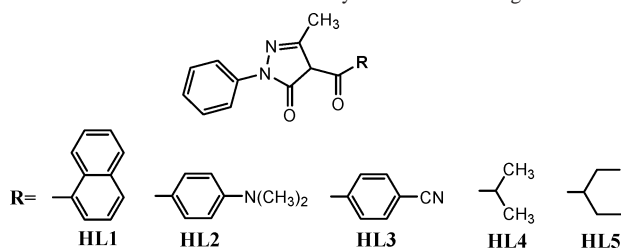
* To whom correspondence should be addressed. E-mail: fyli@fudan.edu.cn (F.L.); chhuang@pku.edu.cn (C.H.). Fax: 86-21-55664621 (F.L., C.H.). Tel: 86-21-55664185 (F.L., C.H.).

[†] Fudan University.

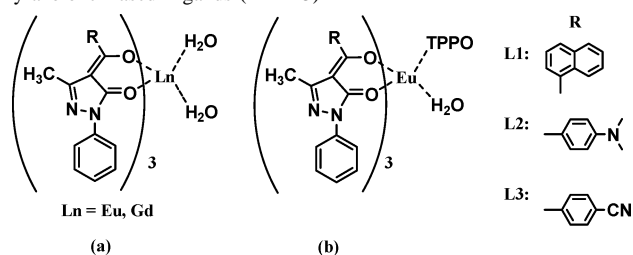
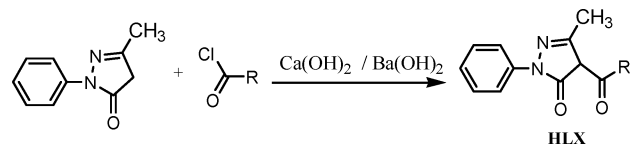
[‡] Northwest University.

- (1) (a) Bünzli, J.-C. G. In *Lanthanide Probes in Life, Chemical and Earth Sciences*; Bünzli, J.-C. G., Choppin, G. R., Eds.; Elsevier: Amsterdam, 1989. (b) Huang, C. H.; Ed. *Coordination Chemistry of Rare Earth Complexes*; Science Press: Beijing, 1997; and references therein.
- (2) (a) Hemmila, I. A., Ed. *Applications of Fluorescence in Immunoassays*; Wiley: New York, 1991. (b) Cha, A.; Snyder, G. E.; Selvin, P. R.; Bezanilla, F. *Nature* **1999**, *402*, 809 and references therein.
- (3) (a) Montalti, M.; Prodi, L.; Zaccaroni, N.; Charbonnière, L.; Douce, L.; Zissel, R. *J. Am. Chem. Soc.* **2001**, *123*, 12694. (b) Mahajan, R. K.; Kaur, I.; Kaur, R.; Uchida, S.; Onimaru, A.; Shinoda, S.; Tsukube, H. *Chem. Commun.* **2003**, 2238. (c) Atkinson, P.; Bretonniere, Y.; Parker, D. *Chem. Commun.* **2004**, 438. (d) Gunnlaugsson, T.; Leonard, J. P.; Sénéchal, K.; Harte, A. *J. Chem. Commun.* **2004**, 782 and references therein.

- (4) Sinha, S. P. *Complexes of the Rare Earth*; Pergamon: London, 1966.
- (5) Kido, J.; Okamoto, Y. *Chem. Rev.* **2002**, *102*, 2357.
- (6) (a) Wang, J.; Wang, R.; Yang, J.; Zheng, Z.; Carducci, M. D.; Cayon, T.; Peyghambarian, N.; Jabbour, G. E. *J. Am. Chem. Soc.* **2001**, *123*, 6179. (b) Bassett, A. P.; Magennis, S. W.; Glover, P. B.; Lewis, D. J.; Spencer, N.; Parsons, S.; Williams, R. M.; De Cola, L.; Pikramenou, Z. *J. Am. Chem. Soc.* **2004**, *126*, 9413 and references therein.
- (7) Gao, X. C.; Cao, H.; Huang, C. H.; Li, B. G.; Umitani, S. *Appl. Phys. Lett.* **1998**, *72*, 2217.
- (8) (a) Xin, H.; Li, F. Y.; Shi, M.; Bian, Z. Q.; Huang, C. H. *J. Am. Chem. Soc.* **2003**, *125*, 7166. (b) Xin, H.; Shi, M.; Zhang, X. M.; Li, F. Y.; Bian, Z. Q.; Ibrahim, K.; Liu, F. Q.; Huang, C. H. *Chem. Mater.* **2003**, *15*, 3728.
- (9) (a) Kido, J.; Nagai, K.; Okamoto, Y.; Skothen, T.; Yamagata, Y. *Chem. Lett.* **1991**, 1267. (b) Adachi, C.; Baldo, M. A.; Forrest, S. R. *J. Appl. Phys.* **2000**, *87*, 8049. (c) Oyamada, T.; Kawamura, Y.; Koyama, T.; Sasabe, H.; Adachi, C. *Adv. Mater.* **2004**, *16*, 1082.

Chart 1. Molecular Structures of the Pyrazolone-Based Ligands

1,3-propanedione (HDBM) and α -thenoyltrifluoroacetone (HTTA).^{9–14} However, the electroluminescent properties of these europium complexes¹³ have not been as satisfactory as those of the terbium complexes⁸ up to now. One of the important reasons is the poor carrier transporting property of these europium complexes.^{5,8,18} In our previous study, we noticed that the pyrazolone-based ligands (**HL4**)⁷ and (**HL5**)⁸ with an alkyl group at the 4-position of pyrazolone ring not only have suitable triplet energy levels matching 5D_4 (20 400 cm^{-1}) of Tb^{3+} but also have good carrier transporting properties. The OLED device based on tris[1-phenyl-3-methyl-4-(2-ethylbutyl)-5-pyrazolonato](triphenylphosphine oxide)terbium [$\text{Tb}(\text{L5})_3(\text{TPPO})$] exhibited good electroluminescent properties (11 lm W^{-1}).⁸ However, the triplet energy level of **HL5** is too high for the 5D_0 (17 500 cm^{-1}) energy level of Eu^{3+} , so that this ligand is not suitable to be used as a sensitizer for europium(III) ion. To reduce the triplet energy level of the pyrazolone-based ligand, herein, 1-phenyl-3-methyl-4-(1-naphthoyl)-5-pyrazolone (**HL1**), 1-phenyl-3-methyl-4-(4-(dimethylamino)benzoyl)-5-pyrazolone (**HL2**) and 1-phenyl-3-methyl-4-(4-cyanobenzoyl)-5-pyrazolone (**HL3**) (see Chart 1) were synthesized by introducing electron-poor or electron-rich aryl substituents into the 4-position of the pyrazolone ring. Their corresponding lanthanide ($\text{Ln} = \text{Eu}, \text{Gd}$) complexes (see Chart 2) were

Chart 2. Molecular Structures of the Eu(III) Complexes with the Pyrazolone-Based Ligands (**L1–L3**)**Scheme 1.** Synthesis Route of the Pyrazolone Ligands

obtained and investigated by measuring their photophysical properties.

Experimental Section

Materials and Apparatus. 2,9-Dimethyl-4,7-diphenyl-1,10-phenanthroline (BCP), 1-phenyl-3-methyl-5-pyrazolone, 4-*N,N*-dimethylaminobenzoyl chloride, 4-cyanobenzoyl chloride, and 1-naphthoyl chloride were obtained from Acros. *N,N'*-Diphenyl-*N,N'*-bis(1-naphthyl)-1,1'-diphenyl-4,4'-diamine (NPB) was purchased from Aldrich. Tris(8-hydroxyquinolino)aluminum (AlQ) was synthesized in our laboratory and sublimed twice before use. The lanthanide oxides were purchased from Shanghai Yuelong Co., Ltd., and the lanthanide nitrate hexahydrates were synthesized in our laboratory. Indium tin oxide (ITO) glass substrate with a sheet resistance of 15 Ω/\square was kindly supplied by China Southern Glass Holding Co. Ltd.

The photoluminescence spectra were measured on an Edinburgh LFS920 fluorescence spectrophotometer. UV–visible absorption spectra were recorded using a Shimadzu 3000 UV–vis–NIR spectrophotometer. NMR spectra were recorded on Mercury Plus 400NB NMR spectrometer. The luminance–current–voltage ($B-I-V$) curves were measured with a computer-controlled Keithley 2400 sourcemeter unit with a calibrated silicon diode. The EL luminescence and chromaticity values were measured using a Photo Research PR-650 spectrophotometer. The element analyses were performed with VarioEL III O-Element analyzing system. Fluorescence lifetime was recorded on a single photon counting spectrometer from Edinburgh Instruments (FLS920) with microsecond pulse lamp as the excitation source. The data were analyzed by iterative convolution of the luminescence decay profile with the instrument response function using a software package provided by Edinburgh Instruments.

General Procedure for Synthesis of the Ligands. The ligands (**HL1–HL3**) were synthesized according to the method reported previously¹⁹ (see Scheme 1). 1-Phenyl-3-methyl-5-pyrazolone (0.05 mol) and 150 mL of dried 1,4-dioxane were placed in a 50 mL flask with a magnetic stirrer and heated at 70 $^{\circ}\text{C}$ for 10 min. To the resulting yellow solution, calcium hydroxide (0.12 mol) and barium hydroxide (0.03 mol) in small portions were added, and then the corresponding acyl chloride (0.058 mol) was added dropwise. The resulting mixture was heated to reflux for 24 h. The cloudy yellowish mixture was cooled to room temperature and

- (10) (a) Fang, J. F.; Ma, D. G. *Appl. Phys. Lett.* **2003**, *83*, 4041. (b) Liang, F. S.; Zhou, Q. G.; Cheng, Y. X.; Wang, L. X.; Ma, D. G.; Jing, X. B.; Wang, F. S. *Chem. Mater.* **2003**, *15*, 1935. (c) Zhu, X.-H.; Wang, L.-H.; Ru, J.; Huang, W.; Fang, J.-F.; Ma, D.-G. *J. Mater. Chem.* **2004**, *14*, 2732.
- (11) (a) Sun, M.; Xin, H.; Wang, K. Z.; Zhang, Y. A.; Jin, L. P.; Huang, C. H. *Chem. Commun.* **2003**, 702. (b) Guan, M.; Bian, Z. Q.; Li, F. Y.; Xin, H.; Huang, C. H. *New J. Chem.* **2003**, *27*, 1731. (c) Xin, H.; Li, F. Y.; Guan, M.; Huang, C. H.; Sun, M.; Wang, K. Z.; Zhang, Y. A.; Jin, L. P. *J. Appl. Phys.* **2003**, *94*, 4729. (d) Huang, L.; Wang, K. Z.; Huang, C. H.; Li, F. Y.; Huang, Y. Y. *J. Mater. Chem.* **2001**, *11*, 790.
- (12) Hu, W. P.; Matsumura, M.; Wang, M. Z.; Jin, L. P. *Appl. Phys. Lett.* **2000**, *39*, 4271.
- (13) (a) Sun, P.-P.; Duan, J.-P.; Shih, H.-T.; Cheng, C.-H. *Appl. Phys. Lett.* **2002**, *81*, 792. (b) Sun, P. P.; Duan, J.; Lih, J.; Cheng, C. *Adv. Funct. Mater.* **2003**, *13*, 683.
- (14) Liang, C. J.; Zhao, D.; Hong, Z. R.; Zhao, D. X.; Liu, X. Y.; Li, W. L.; Peng, J. B.; Yu, J. Q.; Lee, C. S.; Lee, S. T. *Appl. Phys. Lett.* **2000**, *76*, 67.
- (15) Yu, J. B.; Zhou, L.; Zhang, H. J.; Zheng, Y. X.; Li, H. R.; Deng, R. P.; Peng, Z. P.; Li, Z. F. *Inorg. Chem.* **2005**, *44*, 1611.
- (16) McGehee, M. D.; Bergstedt, T.; Zhang, C.; Saab, A. P.; O'Regan, M. B.; Bazan, G. C.; Srdanov, V. I.; Heeger, A. J. *Adv. Mater.* **1999**, *11*, 1349. (b) Robinson, M. R.; O'Regan, M. B.; Bazan, G. C. *Chem. Commun.* **2000**, 1645.
- (17) Okada, K.; Wang, Y. F.; Chen, T. M.; Kitamura, M.; Nakaya, T.; Inoue, H. *J. Mater. Chem.* **1999**, *9*, 3023.
- (18) Pettinari, C.; Marchetti, F.; Cingolani, A.; Drozdov, A.; Timokhin, I.; Troyanov, S. I.; Tsaryuk, V.; Zolin, V. *Inorg. Chim. Acta* **2004**, *357*, 4181.

- (19) Li, H.; Huang, C. H.; Zhou, Y. F.; Zhao, X. S.; Xia, X. H.; Li, T. K.; Bai, J. *J. Mater. Chem.* **1995**, *5*, 1871.

poured into a 350 mL solution of ice-cold hydrochloric acid (3 mol L⁻¹) under stirring. The yellow precipitate was filtered and recrystallized from acetone and water.

1-Phenyl-3-methyl-4-(1-naphthoyl)-5-pyrazolone (HL1). Yield: 62%. Mp: 167–169 °C. ¹H NMR (DMSO, 400 MHz, TMS): δ 8.039 (d, *J* = 7.2 Hz, 1H; ph-H), 8.002 (d, *J* = 6.8 Hz, 1H; ph-H), 7.953 (d, *J* = 7.2 Hz, 1H; ph-H), 7.661 (d, *J* = 7.2 Hz, 2H; ph-H), 7.583 (m, 4H; ph-H), 7.464 (t, *J* = 6.4 Hz, 2H; ph-H), 7.296 (t, *J* = 7.6 Hz, 1H; ph-H), 1.879 (s, 3H, CH₃). ¹³C NMR (CDCl₃): δ 193.1, 161.2, 148.9, 137.4, 135.6, 133.7, 131.2, 129.9, 129.4, 128.8, 127.7, 127.0, 126.9, 125.6, 125.1, 125.0, 121.0, 105.6, 14.9.

1-Phenyl-3-methyl-4-(4-dimethylaminobenzoyl)-5-pyrazolone (HL2). Yield: 55%. Mp: 194–195 °C. ¹H NMR (CDCl₃, 400 MHz, TMS): δ 7.911 (d, *J* = 8 Hz, 2H; ph-H), 7.656 (d, *J* = 8 Hz, 1H; ph-H), 7.456 (t, *J* = 6 Hz, 2H; ph-H), 7.268 (t, *J* = 5.2 Hz, 1H; ph-H), 6.740 (d, *J* = 7.6 Hz, 2H; ph-H), 3.088 (s, 6H; N-CH₃), 2.298 (s, 3H; CH₃). ¹³C NMR (CDCl₃): δ 188.5, 163.5, 153.5, 147.8, 138.0, 131.3, 129.2, 126.3, 123.2, 120.6, 110.9, 103.1, 40.3, 17.0.

1-Phenyl-3-methyl-4-(4-cyanobenzoyl)-5-pyrazolone (HL3). Yield: 78%. Mp: 177–179 °C. ¹H NMR (CDCl₃, 400 MHz, TMS): δ 7.835 (m, 4H; ph-H), 7.738 (d, *J* = 8 Hz, 2H; ph-H), 7.485 (t, *J* = 7.6 Hz, 2H; ph-H), 7.337 (t, *J* = 7.6 Hz, 1H; ph-H), 2.048 (s, 3H; CH₃). ¹³C NMR (CDCl₃): δ 191.1, 160.9, 147.4, 142.1, 137.1, 132.6, 129.5, 128.5, 127.4, 121.2, 118.1, 110.0, 103.7, 15.9.

Synthesis of the Complexes. The Eu(III) and Gd(III) complexes with the ligands **HL1–HL3** were synthesized according to the method reported previously.⁸

Eu(L1)₃(H₂O)₂, Tris[1-phenyl-3-methyl-4-(1-naphthoyl)-5-pyrazolonato]europium Dihydrate. A 1.0 mmol amount of Eu(NO₃)₃·6H₂O was added to an ethanol solution containing 3.0 mmol of **HL1** under stirring, and the pH was adjusted to ca. 5 by dropwise adding of 3.0 mmol NaOH. The solution was stirred for 5 h to obtain the yellow solid product, which was washed using deionized water and dried. Anal. Calcd for C₆₃H₄₉EuN₆O₈: C, 64.67; H, 4.22; N, 7.18. Found: C, 64.85; H, 4.20; N, 7.25.

The other complexes were prepared and purified by the same procedure.

Eu(L2)₃(H₂O)₂, Tris[1-phenyl-3-methyl-4-(4-(dimethylamino)benzoyl)-5-pyrazolonato]europium Dihydrate. Anal. Calcd for C₅₇H₅₈EuN₉O₈: C, 59.58; H, 5.09; N, 10.97. Found: C, 59.33; H, 5.34; N, 10.52.

Eu(L3)₃(H₂O)₂, Tris[1-phenyl-3-methyl-4-(4-cyanobenzoyl)-5-pyrazolonato]europium Dihydrate. Anal. Calcd for C₅₄H₄₀EuN₉O₈: C, 59.24; H, 3.68; N, 11.51. Found: C, 58.57; H, 3.82; N, 11.43.

Gd(L1)₃(H₂O)₂, Tris[1-phenyl-3-methyl-4-(1-naphthoyl)-5-pyrazolonato]gadolinium Dihydrate. Anal. Calcd for C₆₃H₄₉GdN₆O₈: C, 64.38; H, 4.20; N, 7.15. Found: C, 64.75; H, 4.18; N, 7.11.

Gd(L2)₃(H₂O)₂, Tris[1-phenyl-3-methyl-4-(4-(dimethylamino)benzoyl)-5-pyrazolonato]gadolinium Dihydrate. Anal. Calcd for C₅₇H₅₈GdN₉O₈: C, 59.31; H, 5.06; N, 10.92. Found: C, 59.82; H, 4.93; N, 11.45.

Gd(L3)₃(H₂O)₂, Tris[1-phenyl-3-methyl-4-(4-cyanobenzoyl)-5-pyrazolonato]gadolinium Dihydrate. Anal. Calcd for C₅₄H₄₀GdN₉O₈: C, 58.95; H, 3.66; N, 11.46. Found: C, 58.34; H, 3.74; N, 11.03.

Eu(L1)₃(TPPO)(H₂O), Tris[1-phenyl-3-methyl-4-(1-naphthoyl)-5-pyrazolonato](triphenylphosphine oxide)europium Hydrate. A 1.0 mmol amount of Eu(NO₃)₃·6H₂O was added to an ethanol

Table 1. Crystal Data, Collection, and Structure Refinement Parameters

param	HL2	Eu(L3) ₃ (tppo)(H ₂ O)
empirical formula	C ₁₉ H ₁₈ N ₃ O ₂	C ₇₂ H ₅₃ EuN ₉ O ₈ P
fw	320.36	1355.16
cryst system	monoclinic	triclinic
space group	<i>P</i> 2 ₁ / <i>c</i>	<i>P</i> $\bar{1}$
cryst size	0.20 × 0.10 × 0.05	0.20 × 0.18 × 0.12
<i>a</i> /Å	7.625(2)	14.161(3)
<i>b</i> /Å	17.919(6)	15.122(3)
<i>c</i> /Å	12.219(4)	17.272(4)
α (deg)	90	100.72(3)
β (deg)	106.286	111.64(3)
γ (deg)	90	106.88(3)
<i>V</i> /Å ³	1602.5(9)	3106.0(11)
<i>Z</i>	4	2
ρ _{calcd} /g cm ⁻³	1.328	1.449
μ/mm ⁻¹	0.088	1.102
<i>F</i> (000)	676	1380
R1 [<i>I</i> > 2σ(<i>I</i>)]	0.0587	0.0499
wR2 [<i>I</i> > 2σ(<i>I</i>)]	0.1676	0.1053
R1 (all data)	0.0884	0.0990
wR2 (all data)	0.1863	0.1195
GOF	0.949	0.908

solution containing 3.0 mmol of **HL1** and 1.0 mmol of triphenylphosphine oxide, and after stirring, 3.0 mmol of NaOH was added dropwise with the pH being about 5. The solution was stirred for 5 h to obtain the yellowish solid product. The product was washed using deionized water and dried. Anal. Calcd for C₈₁H₆₂EuN₆O₈P: C, 68.02; H, 4.37; N, 5.88. Found: C, 68.69; H, 4.75; N, 5.33.

Eu(L2)₃(TPPO)(H₂O), Tris[1-phenyl-3-methyl-4-(4-(dimethylamino)benzoyl)-5-pyrazolonato](triphenylphosphine oxide)europium Hydrate. Anal. Calcd for C₇₅H₇₁EuN₉O₈P: C, 63.92; H, 5.08; N, 8.94. Found: C, 64.10; H, 5.34; N, 8.58.

Eu(L3)₃(TPPO)(H₂O), Tris[1-phenyl-3-methyl-4-(4-cyanobenzoyl)-5-pyrazolonato](triphenylphosphine oxide)europium Hydrate. Anal. Calcd for C₇₂H₅₃EuN₉O₈P: C, 63.81; H, 3.94; N, 9.30. Found: C, 64.23; H, 3.94; N, 8.99.

Crystallography. The crystals of **HL2** and **Eu(L3)₃(TPPO)(H₂O)** were mounted on glass fibers and transferred to a Bruker SMART CCD area detector. Crystallographic measurements were carried out using a Bruker SMART CCD diffractometer, with σ scans and graphite-monochromated Mo K α radiation (λ = 0.710 73 Å), at room temperature. The structures were solved by direct methods and refined by full-matrix least-squares on *F*² values using the program SHELXS-97.²⁰ All non-hydrogen atoms were refined anisotropically. Hydrogen atoms were calculated in ideal geometries. For the full-matrix least-squares refinements [*I* > 2σ(*I*)], the unweighted and weighted agreement factors of R1 = Σ(*F*_o - *F*_c)/Σ*F*_o and wR2 = [Σw(*F*_o² - *F*_c²)/Σw*F*_o⁴]^{1/2} were used. The crystal data and details of the structure determinations are summarized in Table 1. CCDC reference nos.: 225972 for **HL2** and 271332 for **Eu(L3)₃(TPPO)(H₂O)**.

Preparation of EL Devices. Electroluminescent devices based on the europium complex were fabricated through vacuum deposition of the materials onto clean glass precoated with a layer of indium tin oxide at 10⁻⁵ Pa. The rates of deposition of each organic compound were 1–2 Å s⁻¹ and for the europium complex were 0.1–0.2 Å s⁻¹. The cathode was formed through coevaporation of Mg and Ag with Mg:Ag ratio of 10:1, followed by vacuum deposition of Ag (80 nm). The emitting diode has an effective area of 4.0 mm². The thickness of the deposited layer and the evaporation

(20) Sheldrick, G. M. *SHELXTL-Plus V5.1 software Reference Manual*; Bruker AXS Inc.: Madison, WI, 1997.

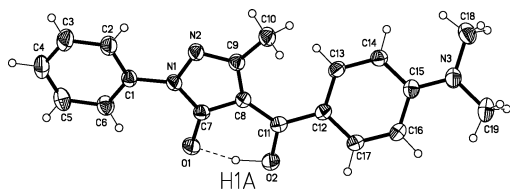


Figure 1. ORTEP diagram of **HL2** with the thermal ellipsoids drawn at the 30% probability level.

speed of the individual materials were monitored in a vacuum with quartz crystal monitors.

Results and Discussion

Synthesis and Characterization of the Ligands. 1-Phenyl-3-methyl-4-(*R*)-5-pyrazolone ligands (**HLX**, *X* = 1–3) were prepared according to Scheme 1 and characterized by NMR. The resulting compounds are soluble in ethanol, chloroform, acetonitrile, and dimethyl sulfoxide. No obvious ^1H NMR signals of the hydrogen atom linked to the carbon atom of the pyrazolone ring were observed for all ligands, indicating that the enol configuration of β -diketonate formed.^{1b} This conclusion was confirmed further by the crystallographic data for the ligand **HL2**.

The crystallographic data for **HL2** are listed in Table 1. An ORTEP diagram for the common repeating unit is shown in Figure 1. The molecular structure of **HL2** reveals a planar arrangement of non-hydrogen atoms (O2, C11, C8, C7, O1, mean deviation of 0.0362 Å), and H1A lies 0.0318 Å from this plane. The carbonyl bond lengths for C11–O2 and C7–O1 are 1.30(5) and 1.28(7) Å, respectively. There is an intramolecular hydrogen bond between the atoms O1 and O2 (O2–H1A...O1, 2.529 Å, 160.3°). These data suggest that, in the ring consisting of O1/O2, the enolic proton is not shared symmetrically with the carbonyl oxygens; that is, **HL2** exists in the enol form in the solid state. Although the phenyl plane consisting of C1–C6 and the pyrazolone ring (mean deviation of 0.0632 Å) are almost in a plane, in which the dihedral angle is 5.2°, the whole molecule is not coplanar, and the dihedral angle between the pyrazolone ring and the phenyl plane consisting of C12–C17 is 42.5°.

Structure Characterization of Eu(L3)₃(TPPO)(H₂O). The structure of Eu(L3)₃(TPPO)(H₂O) was characterized by X-ray crystallography. Details of the crystal data and data collection parameters for Eu(L3)₃(TPPO)(H₂O) are given in Table 1. An ORTEP diagram for the asymmetric unit of Eu(L3)₃(TPPO)(H₂O) is shown in Figure 2. The coordination geometry of the metal center is best described as a distorted bicapped trigonal prism with the trigonal prism being composed of six oxygen atoms (O1, O2, O3, O5, O6, O8). Among them, O1, O2 and O5, O6 are from two β -diketonates, and O3 and O8 are from the third diketone and a water molecule, respectively. Another two oxygen atoms (O4, O7) cap the two quadrilateral faces O3–O5–O8–O1 and O2–O6–O3–O1, respectively. The average Eu–O distance is 2.39(6) Å [2.34(4)–2.49(0) Å], which is little smaller than the sum of the radii of Eu³⁺ (1.07 Å, eight coordinated) and O²⁻ (1.42 Å).^{1b} It is noted that, in this complex, the bichelate rings are coplanar. The bond lengths between the oxygen

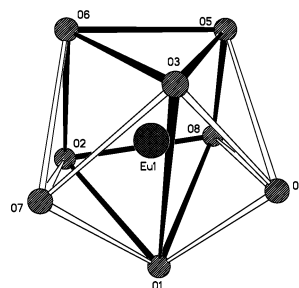
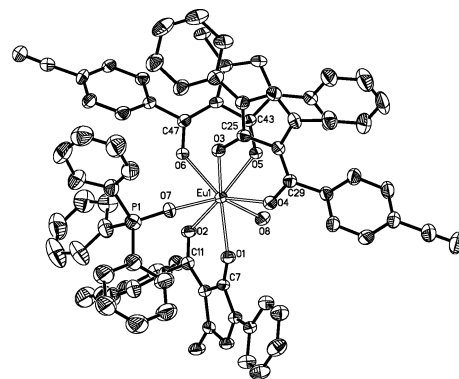


Figure 2. ORTEP diagram of Eu(L3)₃(TPPO)(H₂O) with the thermal ellipsoids drawn at the 30% probability level and the H atoms removed for clarity.

and the carbon atoms of the β -diketonate anions are almost unified (1.26(3), 1.24(8), 1.26(5), 1.26(6), 1.26(9), and 1.26(2) Å corresponding to O1–C7, O2–C11, O3–C25, O4–C29, O5–C43, and O6–C47, respectively), implying that strong conjugation exists in the chelate rings.

UV–Vis Spectra. UV–vis absorption spectra of the ligands (**HL1**–**HL3**) and their corresponding Eu(III) complexes are shown in Figure 3. The maximum absorption bands at 282, 350, and 293 nm for the ligands **HL1**–**HL3**, respectively, are attributed to singlet–singlet π – π^* enol absorption of β -diketonates. Compared with the ligand **HL4** ($\lambda_{\text{max}} = 262$ nm), the absorption peaks are red-shifted 20, 88, and 31 nm for **HL1**–**HL3**, respectively. Interestingly, the UV–vis maximum band is red-shifted to 350 nm for **HL2**, indicating that the conjugation degree enlarges and the π – π^* energy level is lowered by introduction of the *N,N*-dimethylaminobenzoyl group. Furthermore, compared with the spectra of the ligands **HL1**–**HL3**, the first absorption bands of the corresponding europium complexes are all red-shifted 6–10 nm, which is a consequence of the enlargement of the conjugate structure of ligands after coordinating to the lanthanide ion. The spectral shapes of the Eu(III) complexes in CHCl₃ are similar to those of the corresponding ligands, indicating that the coordination of the europium ion does not significantly influence the energy of the singlet state of the β -diketonate ligands. The molar absorption coefficients (ϵ) of **HL1**–**HL3** are calculated as 1.8×10^4 (282 nm), 1.9×10^4 (350 nm), and 1.3×10^4 (293 nm) L·mol⁻¹·cm⁻¹, respectively, revealing that these ligands have a strong ability of absorbing light. Similarly, the determined molar absorption coefficients (ϵ) of the complexes Eu(LX)₃(H₂O)₂ (*X* = 1–3) were 6.1×10^4 (288 nm), 5.5×10^4 (360 nm), and 3.5×10^4 (301 nm) L·mol⁻¹·cm⁻¹, respectively, which are about

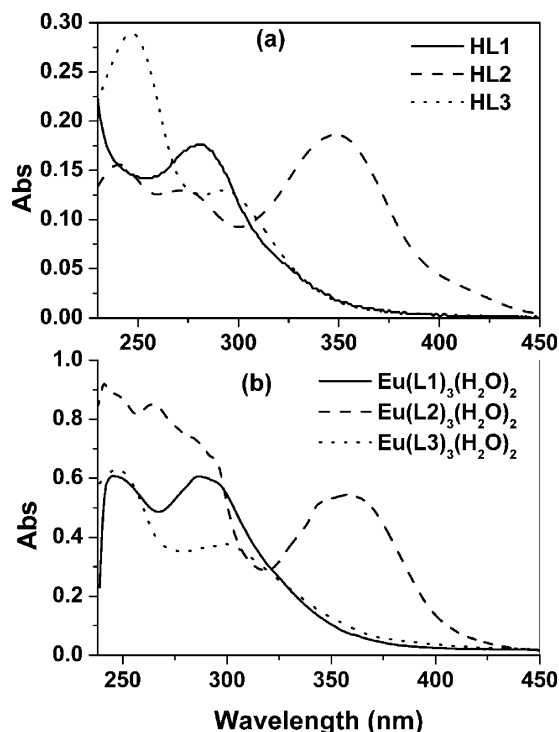


Figure 3. Absorption spectra of the ligands (a) and their Eu(III) complexes (b) in CHCl_3 solution ($c = 1.0 \times 10^{-5}$ M).

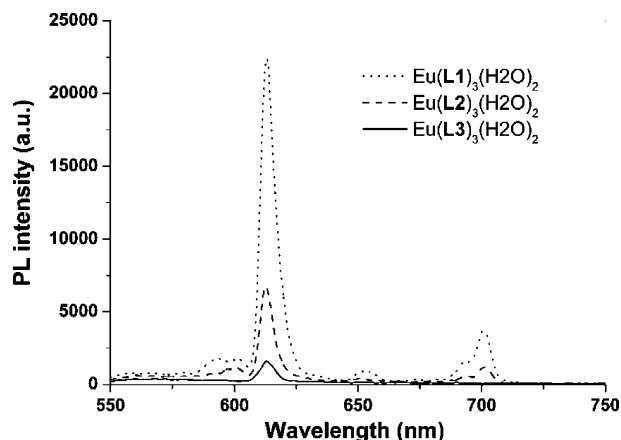


Figure 4. Luminescence spectra of $\text{Eu}(\text{LX})_3(\text{H}_2\text{O})_2$ ($X = 1-3$) at 298 K. The intensities are relative to the fluorescence intensity of $\text{Eu}(\text{L1})_3(\text{H}_2\text{O})_2$.

three times of those of the corresponding ligands, indicating the presence of three ligands/complex molecule.

Fluorescence Spectra. The red luminescence, characteristic of ${}^5\text{D}_0 \rightarrow {}^7\text{F}_j$ ($J = 0-4$) emission bands of Eu^{3+} was observed when $\text{Eu}(\text{LX})_3(\text{H}_2\text{O})_2$ ($X = 1-3$) were excited at 290 nm (see Figure 4). However, the fluorescent intensities of these complexes are different. The excitation spectra of $\text{Eu}(\text{L1})_3(\text{H}_2\text{O})_2$, $\text{Eu}(\text{L2})_3(\text{H}_2\text{O})_2$, and $\text{Eu}(\text{L3})_3(\text{H}_2\text{O})_2$ with band maxima at 284, 349, and 295 nm, respectively, match the corresponding absorption spectra, confirming that energy transfer takes place from the ligands to Eu^{3+} ion. We also investigated the emission spectra of the complexes $\text{Eu}(\text{LX})_3(\text{H}_2\text{O})_2$ ($X = 1-3$) in the different solvents, such as CH_3CN , CHCl_3 , DMF, and DMSO. The similarity of the emission patterns in these solvents suggests that there are no solvent-dependent structural changes in the complexes.

Photophysical Properties of the Complexes. The data for photophysical properties for $\text{Eu}(\text{LX})_3(\text{H}_2\text{O})_2$ ($X = 1-3$) are shown in Table 2. The overall luminescent quantum yields (ϕ_{overall}) of these europium complexes were measured using Rhodamine B in ethanol (2.0×10^{-5} mol/L, $\phi_{\text{ref}} = 0.69$)²¹ as a reference and were calculated according to the well-known method given

$$\phi_{\text{overall}} = \frac{n^2 A_{\text{ref}} I}{n_{\text{ref}}^2 A I_{\text{ref}}} \phi_{\text{ref}} \quad (1)$$

Here n , A , and I denote the refractive index of solvent, the area of the emission spectrum, and the absorbance at the excitation wavelength, respectively. Subscript ref denotes the reference, and no subscript denotes the unknown sample. The refractive index is assumed to be equivalent to that of the pure solvent: 1.361 for ethanol and 1.344 for CH_3CN at room temperature. The overall fluorescent quantum yields (ϕ_{overall}) of $\text{Eu}(\text{L1})_3(\text{H}_2\text{O})_2$, $\text{Eu}(\text{L2})_3(\text{H}_2\text{O})_2$, and $\text{Eu}(\text{L3})_3(\text{H}_2\text{O})_2$ were calculated as 9.2×10^{-3} , 3.1×10^{-3} , and 4.0×10^{-4} , respectively, revealing that the structural change of the ligands affects the fluorescent quantum yields of the Eu-(III) complexes.

The luminescence lifetimes (τ) were also investigated for these complexes except for $\text{Eu}(\text{L3})_3(\text{H}_2\text{O})_2$ due to its very weak fluorescent intensity. The measured luminescent decays (see ESI) of $\text{Eu}(\text{L1})_3(\text{H}_2\text{O})_2$ and $\text{Eu}(\text{L2})_3(\text{H}_2\text{O})_2$ can be described by monoexponential kinetics, which suggests that in these complexes only one species exists in the excited state. In combination with the data for the fluorescent intensities, the data for the fluorescent lifetimes show that the higher the fluorescent intensities, the longer the fluorescent lifetimes are for the complexes (see Table 2). According to the above results of fluorescence and phosphorescence properties of the europium complexes, we can conclude that the modification of the ligands is effective.

To understand the effect of the ligand modification on the fluorescence properties of $\text{Eu}(\text{LX})_3(\text{H}_2\text{O})_2$ ($X = 1-3$), the efficiency of energy transfer (ϕ_{transfer}) from the ligand to Eu^{3+} and the probability of the europium emission (ϕ_{Ln}) were investigated on the basis of the method developed by Selvin et al.²² The overall quantum yield (ϕ_{overall}) of the europium complex treats the complex as a “black box” where internal processes are not explicitly considered: given that complex absorbs a photon (i.e. the antenna is excited), the overall quantum yield can be defined as

$$\phi_{\text{overall}} = \phi_{\text{transfer}} \phi_{\text{Ln}} \quad (2)$$

When a lanthanide chelate is mixed with an acceptor of known quantum yield and very short fluorescence lifetime (ns), the efficiency of energy transfer between them (ϕ_{ET}) and the probability of lanthanide emission (ϕ_{Ln}) are calculated from both fluorescence decay lifetime and intensity measure-

(21) Filipescu, N.; Mushrush, G. W.; Hurt, C. R.; McAvoy, N. *Nature* **1966**, *211*, 960.

(22) Xiao, M.; Selvin, P. *J. Am. Chem. Soc.* **2001**, *123*, 7067 and references therein.

Table 2. Photophysical Properties of Eu(LX)₃(H₂O)₂ (X = 1–3) in Acetonitrile

compd	$\lambda_{\max}^{\text{abs}}/\text{nm}$ ($10^{-4}\epsilon/\text{dm}^3\text{mol}^{-1}\text{cm}^{-1}$)	S_1/cm^{-1}	$\lambda_{\max}^{\text{phos}}/\text{nm}^b$	T_1/cm^{-1}	$\lambda_{\max}^{\text{PL}}/\text{nm}^c$	$\tau/\mu\text{s}$ (χ^2) ^c	ϕ_{overall} ($\times 10^3$)	$\phi_{\text{Ln}}/\%$	$\phi_{\text{transfer}}/\%$	$k_{\text{rad}}/\text{s}^{-1}$	$10^{-4}k_{\text{nr}}/\text{s}^{-1}$
Eu(L1) ₃ (H ₂ O) ₂	288 (6.1)	~28 900	554	~19 600	614	31.50 (1.10)	9.2	2.6	35.1	835	3.13
Eu(L2) ₃ (H ₂ O) ₂	360 (5.5)	~24 450	525	~19 900	614	18.57 (1.12)	3.1	1.9	16.1	1050	5.28
Eu(L3) ₃ (H ₂ O) ₂	301 (3.5)	~27 027	593	~18 200	614		0.4				
Eu(L4) ₃ (H ₂ O) ₂	265 (3.5)	~32 785	460	~23 500							

^a S_1 : singlet energy level. T_1 : triplet energy level. χ^2 is called the “reduced chi-square”. ^b Emission band maximum at 77 K. ^c Emission band maximum and decay lifetimes in CH₃CN solution at room temperature.

ments as the following:

$$\phi_{\text{ET}} = 1 - (\tau_{\text{da}}/\tau_{\text{d}}) \quad (3)$$

$$\phi_{\text{Ln}} = \phi_{\text{a}}(I_{\text{da}}/I_{\text{ad}})/(1/\phi_{\text{ET}} - 1) = \phi_{\text{a}}I_{\text{da}}(\tau_{\text{d}} - \tau_{\text{ad}})/(I_{\text{ad}}\tau_{\text{ad}}) \quad (4)$$

Here ϕ_{a} is the fluorescence quantum yield of the acceptor, τ_{ad} and τ_{d} are the lanthanide complex's excited-state lifetime in the presence and absence of the acceptor respectively, I_{da} is the area under the residual lanthanide emission in the presence of the acceptor, and I_{ad} is the area of the fluorescent emission part of the acceptor.

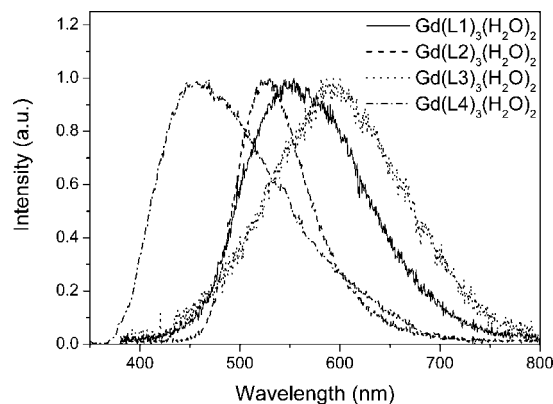
Here, the acceptor was Rhodamine B in acetonitrile, $\phi = 0.52$ and $\tau < 10$ ns. For example, in a mixture solution consisted of 10 μM Eu(L1)₃(H₂O)₂ and 1 μM Rhodamine B, the emission lifetime of the Eu(III) complex ($\lambda_{\text{em}} = 614$ nm) decreased from 31.50 to 29.4 μs , indicating that 6.7% of energy transferred to Rhodamine B. From these measurements and eq 4, the quantum yield (ϕ_{Ln}) of Eu³⁺ in Eu(L1)₃(H₂O)₂ was determined to be 2.6% (in Table 2). Similarly, the other quantum yield (ϕ_{Ln}) of Eu³⁺ was 1.9% for Eu(L2)₃(H₂O)₂ (in Table 2). In combination with the overall quantum yields (ϕ_{overall}) of Eu(L1)₃(H₂O)₂ and Eu(L2)₃(H₂O)₂, we can calculate the efficiency (ϕ_{transfer}) of energy transfer from the ligand to Eu³⁺ according to eq 2. It can be seen from Table 2 that ϕ_{transfer} values of the complexes Eu(L1)₃(H₂O)₂ and Eu(L2)₃(H₂O)₂ were 35.1% and 16.1%, respectively. However, for its very weak fluorescence emission, we did not obtain the quantum yield (ϕ_{Ln}) and the energy transfer efficiency (ϕ_{transfer}) for Eu(L3)₃(H₂O)₂.

With ϕ_{Ln} and τ_{d} determined in acetonitrile, radiative and nonradiative decay rates for the Eu(III) complexes were calculated via the following:

$$k_{\text{rad}} = \phi_{\text{Ln}}/\tau_{\text{d}} \quad k_{\text{nr}} = (1 - \phi_{\text{Ln}})/\tau_{\text{d}} \quad (5)$$

Taking 2.6% of ϕ_{Ln} and 31.50 μs of τ_{d} into account, the radiative and nonradiative decay rates of Eu(L1)₃(H₂O)₂ were 835 and 3.13×10^4 s⁻¹, respectively. Similarly, the radiative and nonradiative decay rates of Eu(L2)₃(H₂O)₂ were 1050 and 5.28×10^4 s⁻¹ (in Table 2), respectively.

To elucidate the energy transfer process of the europium complexes, the energy levels of the relevant electronic states should be estimated. The singlet and triplet energy levels of L1–L3 were estimated by referring to their wavelengths of UV–Vis absorbance edges and the lower wavelength emission edges of the corresponding phosphorescence spectra. It can be seen from Figure 3 that the wavelengths of absorbance

**Figure 5.** Phosphorescent spectra of Gd(LX)₃(H₂O)₂ (X = 1–4) at 77 K.

edge of the ligands **HL1**–**HL3** are 346, 409, and 370 nm, respectively, indicating that their singlet energy levels are ~28 900, 24 450, and 27 027 cm⁻¹, respectively (see Table 2). The triplet energy level of the ligand was not affected significantly by the lanthanide ion, and the lowest lying excited level (⁶P_{7/2} → ⁸S_{7/2}) of Gd(III) is located at 32 150 cm⁻¹.²³ On this basis, the phosphorescence spectra of Gd(LX)₃(H₂O)₂ (X = 1–3) allow one to evaluate the ³ππ* energy levels corresponding ligand anions LX (X = 1–3) for all the lanthanide chelates. The phosphorescence spectra of Gd(L1)₃(H₂O)₂, Gd(L2)₃(H₂O)₂, and Gd(L3)₃(H₂O)₂ at 77 K present their bands with maxima at ca. 554 nm (18 050 cm⁻¹), 525 nm (19 048 cm⁻¹), and 593 nm (16 863 cm⁻¹), respectively, and their energies of zero-phonon transition of the triplet states (³ππ*)²⁴ at about 19 600, 19 900 and 18 200 cm⁻¹, respectively (see Figure 5). Consequently, compared with the triplet energy level (23 500 cm⁻¹) of the ligand **L4** (see Figure 5), the triplet state levels were successfully lowered for the ligands (**L1**–**L3**) with electron-poor or electron-rich aryl substituents at the 4-position of the pyrazolone ring.

Generally, the sensitization pathway in luminescent europium complexes consists of excitation of the ligands into their excited singlet states, subsequent intersystem crossing of the ligands to their triplet states, and energy transfer from the triplet state to the ⁵D_J manifold of the Eu³⁺ ion, following by internal conversion to the emitting ⁵D₀ state; finally, the

(23) (a) Stein, G.; Wurzburg, E. *J. Chem. Phys.* **1975**, *62*, 208. (b) Dieke, G. H. *Spectra and Energy Levels of Rare Earth Ions in Crystals*; Wiley-Interscience: New York, 1968.

(24) (a) Comby, S.; Imbert, D.; Chauvin, A.-S.; Bunzli, J.-C. G.; Charbonniere, L. J.; Ziessel, R. F. *Inorg. Chem.* **2004**, *43*, 7369. (b) Quici, S.; Cavazzini, M.; Marzanni, G.; Accorsi, G.; Armaroli, N.; Ventura, B.; Barigelletti, F. *Inorg. Chem.* **2005**, *44*, 529. (c) Tobita, S.; Arakawa, M.; Tanaka, I. *J. Phys. Chem.* **1985**, *89*, 5649. (d) Prodi, L.; Maestri, M.; Ziessel, R.; Balzani, V. *Inorg. Chem.* **1991**, *30*, 3798.

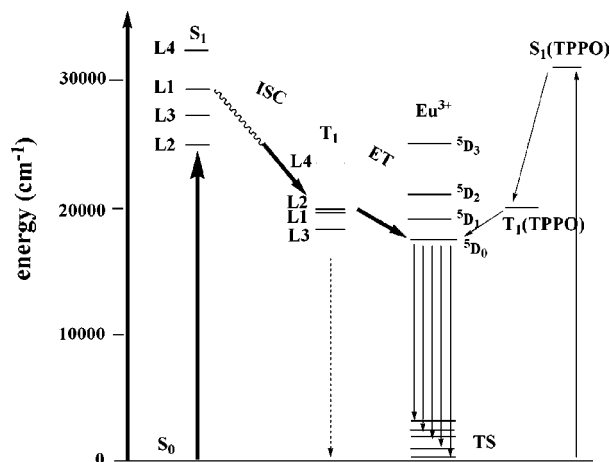


Figure 6. Schematic energy level diagram and the energy transfer process in the systems of $\text{Eu}(\text{LX})_3 \cdot 2\text{H}_2\text{O}$ ($X = 1-3$). S_1 : the first excited singlet state. T_1 : the first excited triplet state.

Eu^{3+} ion emits when transition to the ground state occurs.^{1,25} Moreover, the electron transition from the higher excited states, such as $^5\text{D}_3$ (24 800 cm^{-1}), $^5\text{D}_2$ (21 200 cm^{-1}), and $^5\text{D}_1$ (19 000 cm^{-1}), to $^5\text{D}_0$ (17 500 cm^{-1}) becomes feasible by internal conversion, and most of the photophysical processes take place in this orbital. Consequently, most europium complexes give rise to typical Eu(III) emission bands at ~ 581 , 593, 614, 654, and 702 nm corresponding to the deactivation of the excited state $^5\text{D}_0$ to the ground states $^7\text{F}_J$ ($J = 0-4$). Therefore, the energy level's match of the triplet state of the ligands to $^5\text{D}_0$ of Eu^{3+} is one of the key factors which affects the luminescent properties of the europium complexes.

According to the above experimental results, the schematic energy level diagram and the energy transfer process are shown in Figure 6. The triplet energy levels of **L1** ($\sim 19\,600\text{ cm}^{-1}$), and **L2** ($\sim 19\,900\text{ cm}^{-1}$) are obviously higher than the $^5\text{D}_0$ level (17 500 cm^{-1}) of Eu^{3+} , and their energy gaps $\Delta E(^3\pi\pi^* - ^5\text{D}_0)$ between ligand- and metal-centered levels are $\Delta E > 2000\text{ cm}^{-1}$, too high to allow an effective back energy transfer. According to Latva's empirical rule,²⁶ an optimal ligand-to-metal transfer process for Eu(III) needs $\Delta E(^3\pi\pi^* - ^5\text{D}_0) > 2500\text{ cm}^{-1}$; therefore, the ligand-to-metal transfer processes are effective for $\text{Eu}(\text{L1})_3(\text{H}_2\text{O})_2$ and $\text{Eu}(\text{L2})_3(\text{H}_2\text{O})_2$. We also noticed that the energy gap between the $^1\pi\pi^*$ and $^3\pi\pi^*$ levels are 9300 and 4550 cm^{-1} for the anions **L1** and **L2**, respectively (see Table 2). According to Reinhoudt's empirical rule that the intersystem crossing process becomes effective when $\Delta E(^1\pi\pi^* - ^3\pi\pi^*)$ is at least 5000 cm^{-1} ,²⁷ we believe that the anions **L1** and **L2** (especially **L1**) are suitable as sensitizers for Eu(III) and that the intersystem crossing process of $\text{Eu}(\text{L1})_3(\text{H}_2\text{O})_2$ is more effective than that of $\text{Eu}(\text{L2})_3(\text{H}_2\text{O})_2$. Therefore, it is easy

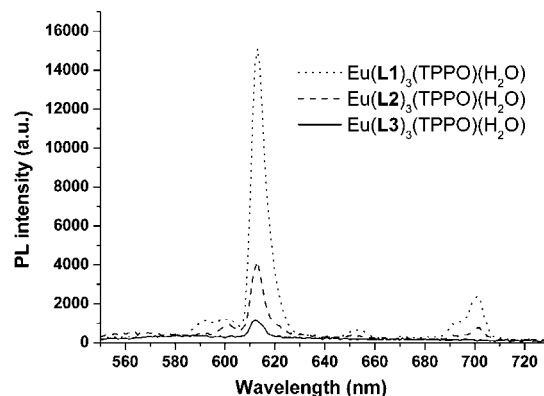


Figure 7. Luminescence spectra of $\text{Eu}(\text{LX})_3(\text{TPPO})(\text{H}_2\text{O})$ ($X = 1-3$) at room temperature. The intensities are relative to the fluorescence intensity of $\text{Eu}(\text{L1})_3(\text{TPPO})(\text{H}_2\text{O})$.

for us to understand that the fluorescent quantum yield of $\text{Eu}(\text{L1})_3(\text{H}_2\text{O})_2$ is higher than that of $\text{Eu}(\text{L2})_3(\text{H}_2\text{O})_2$ (see Table 2). On the contrary, the $^3\pi\pi^*$ state ($\sim 18\,200\text{ cm}^{-1}$) of the anion **L3** is so close to $^5\text{D}_0$ (17 500 cm^{-1}) of Eu(III), giving $\Delta E(^3\pi\pi^* - ^5\text{D}_0) = 700\text{ cm}^{-1}$, too low to prevent thermally competitive back energy transfer from the Eu(III) excited state to the triplet state of **L3**, which predicts that little effective energy transfer takes place from the anion **L3** to Eu(III), resulting in a low fluorescence quantum yield (4.0×10^{-4}) of $\text{Eu}(\text{L3})_3(\text{H}_2\text{O})_2$.

Generally, the method of deoxygenating and reducing temperature becomes feasible to improve the quantum yield of the europium complexes.²⁸ Here, to improve the luminescence intensity, the stronger donor of triphenylphosphine oxide (TPPO)²⁹ with the triplet energy level of $\sim 20\,000\text{ cm}^{-1}$ (see ESI) was introduced to exchange the coordinated water³⁰ and to form the ternary complexes $\text{Eu}(\text{LX})_3(\text{TPPO})(\text{H}_2\text{O})$ ($X = 1-3$). Figure 7 gives the luminescence spectra of $\text{Eu}(\text{LX})_3(\text{TPPO})(\text{H}_2\text{O})$ ($X = 1-3$). Compared to $\text{Eu}(\text{L1})_3(\text{H}_2\text{O})_2$, the quantum efficiency of $\text{Eu}(\text{L1})_3(\text{TPPO})(\text{H}_2\text{O})$ increases about 18%. Similarly, an increase of 24% was obtained for $\text{Eu}(\text{L2})_3(\text{TPPO})(\text{H}_2\text{O})$. Moreover, the fluorescence lifetime was increased to 33.7 μs for $\text{Eu}(\text{L1})_3(\text{TPPO})(\text{H}_2\text{O})$. Since the triplet energy level of TPPO matches the $^5\text{D}_0$ energy level of Eu^{3+} , the energy absorbed by TPPO could be transferred to Eu^{3+} ion directly (see Figure 6), leading to the enhancement of the emission quantum yields of the complexes $\text{Eu}(\text{LX})_3(\text{TPPO})(\text{H}_2\text{O})$ ($X = 1, 2$).

Electroluminescence Properties. For its good luminescent property, the complex $\text{Eu}(\text{L1})_3(\text{TPPO})(\text{H}_2\text{O})$ was used to fabricate the EL devices. No obvious light emission was obtained from the single-layer device A with the configuration of ITO/ $\text{Eu}(\text{L1})_3(\text{TPPO})(\text{H}_2\text{O})$ (60 nm)/Mg:Ag_{10:1} (200 nm)/Ag (80 nm). By using *N,N'*-diphenyl-*N,N'*-bis(1-naphthyl)-1,1'-diphenyl-4,4'-diamine (NPB) and tris(8-hydroxyquinolino)aluminum (AlQ) as hole and electron trans-

(25) (a) Sato, S.; Wada, M. B. *Chem. Soc. Jpn.* **1970**, *43*, 1955. (b) Tanaka, M.; Yamaguchi, G.; Shiokawa, J.; Yamanaka, C. B. *Chem. Soc. Jpn.* **1970**, *43*, 549. (c) Haynes, A. V.; Drickamer, H. G. *J. Chem. Phys.* **1982**, *76*, 114.
 (26) Latva, M.; Takalo, H.; Mukkala, V.-M.; Matachescu, C.; Rodriguez-Ubis, J. C.; Kankare, J. *J. Lumin.* **1997**, *75*, 149.
 (27) Steemers, F. J.; Verboom, W.; Reinhoudt, D. N.; van der Tol, E. B.; Verhoeven, J. W. *J. Am. Chem. Soc.* **1995**, *117*, 9408.

(28) Parker, D.; Dickins, R. S.; Puschmann, H.; Crossland, C.; Howard, J. A. K. *Chem. Rev.* **2002**, *102*, 1977.
 (29) Xin, H.; Shi, M.; Gao, X. C.; Huang, Y. Y.; Gong, Z. L.; Nie, D. B.; Cao, H.; Bian, Z. Q.; Li, F. Y.; Huang, C. H. *J. Phys. Chem. B* **2004**, *108*, 10796.
 (30) Dickins, R. S.; Parker, D.; Bruce, J. I.; Tozer, D. J. *Dalton Trans.* **2003**, 1264.

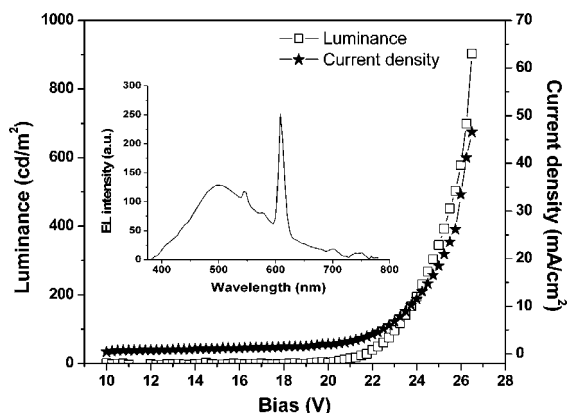


Figure 8. Current density–voltage (★) and luminance–voltage (□) curves of device B with the configuration of ITO/NPB (50 nm)/Eu(L1)₃(TPPO)(H₂O):CBP (6%, 50 nm)/AIQ (40 nm)/Mg:Ag_{10:1} (200 nm)/Ag (80 nm). Inset: EL spectrum (16 V).

porting materials, respectively, and 4,4'-bis(carbazol-9-yl)biphenyl (CBP) as a host material, the three-layer device B with the configuration of ITO/NPB (50 nm)/Eu(L1)₃(TPPO)(H₂O):CBP (6%, 50 nm)/AIQ (40 nm)/Mg:Ag_{10:1} (200 nm)/Ag (80 nm) was fabricated. Figure 8 shows the EL spectrum of the device B. A broad EL emission peaked at 502 nm with a sharp emission peaked at 615 nm and the highest luminance of 920 cd·m⁻² were observed, revealing that the emission of the device B was mainly from AIQ with a small amount of emission from the europium complex. After insertion of hole blocking material 2,9-dimethyl-4,7-diphenyl-1,10-phenanthroline (BCP) between the europium complex and AIQ and improvement of the content of the Eu(III) complex in CBP, device C with the configuration of ITO/NPB (50 nm)/Eu(L1)₃(TPPO)(H₂O):CBP (15%, 50 nm)/BCP (20 nm)/AIQ (20 nm)/Mg:Ag_{10:1} (200 nm)/Ag (80 nm) was fabricated. Its EL spectrum is shown in Figure 9. Device C gave the characteristic emission of the central europium ion, indicating that the carrier recombination zone was well confined in the europium complex layer and their performance was 247 cd·m⁻² at 18.5 V. Current–voltage (*I*–*V*) and luminance–voltage (*L*–*V*) curves of device C are also shown in Figure 9.

Conclusions

In conclusion, we have identified viable operating principles for the modulation of optical properties of the europium complexes by introducing electron-poor or electron-

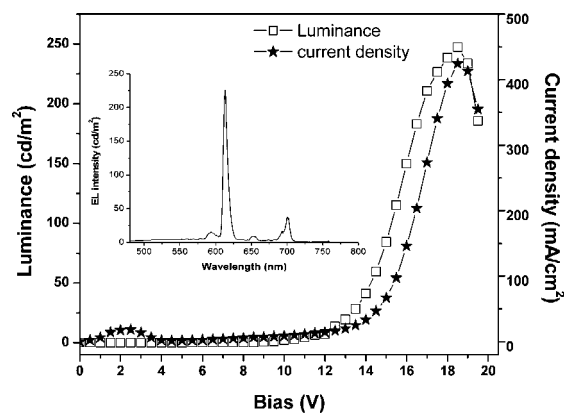


Figure 9. Current–voltage (★) and luminance–voltage (□) curves of device C with configuration of ITO/NPB (50 nm)/Eu(L1)₃(TPPO)(H₂O):CBP (15%, 50 nm)/BCP (20 nm)/AIQ (20 nm)/Mg:Ag_{10:1} (200 nm)/Ag (80 nm). Inset: EL spectrum (18 V).

rich aryl substituents at 4-position of the pyrazolone ring. Three pyrazolone-based ligands HL1–HL3 and their corresponding europium complexes Eu(LX)₃(H₂O)₂ and Eu(LX)₃(TPPO)(H₂O) (*X* = 1–3) were structurally and photophysically characterized. The experiment results prove that the modification of ligands not only alters the triplet state energy but also affects the quantum yield of Eu³⁺ emission and the energy transfer efficiency from the ligand to Eu³⁺, finally resulting in the change of the overall emission quantum yield. The complex Eu(L1)₃(H₂O)₂ at room temperature exhibits 35.1% of energy transfer efficiency (ϕ_{transfer}), 2.6% of probability of lanthanide emission (ϕ_{Ln}), and 9.2×10^{-3} of fluorescent quantum yield, which are the highest values in all europium complexes based on pyrazolone-based ligands up to now. Moreover, we used Eu(L1)₃(TPPO)(H₂O) as the emitter to fabricate successfully an OLED device with a saturated red electroluminescence of 247 cd·m⁻².

Acknowledgment. The authors thank the National Science Foundation of China (Grant 20490210), the NHTRDP (863 Program No. 2002AA302403), and Shanghai Sci. Tech. Comm. (Grants 03QB14006 and 03DZ12031) for financial support.

Supporting Information Available: Data for the crystal structure of HL2 and Eu(L3)₃(TPPO)(H₂O) (CIF), decay lifetimes of Eu(L1)₃(H₂O)₂ and Eu(L2)₃(H₂O)₂, and the phosphorescent spectrum of Gd(NO₃)₃(TPPO)₂. This material is available free of charge via the Internet at <http://pubs.acs.org>.

IC050844P